Asociación Argentina
de Mecánica Computacional

Mecánica Computacional Vol XXXIII, págs. 1529-1541 (artículo completo)
Graciela Bertolino, Mariano Cantero, Mario Storti y Federico Teruel (Eds.)
San Carlos de Bariloche, 23-26 Setiembre 2014

NONLOCAL FREQUENCY ANALYSIS OF NANOSENSORS WITH ATTACHED DISTRIBUTED BIOMOLECULES WITH DIFFERENT BOUNDARY CONDITIONS

Maria A. De Rosa[a], Claudio Franciosi[a], Maria Lippiello[b] and Marcelo T. Piovan[c]

[c]*School of Engineering, University of Basilicata, Viale dell'Ateneo Lucano 10, 85100 Potenza, Italy, maria.derosa@unibas.it, http://www.unibas.it*

[b]*Department of Structures for Engineering and Architecture, University of Naples, Via Forno Vecchio 36, 80134 Naples, Italy, maria.lippiello@unina.it, http://www.unina.it*

[c]*Centro de Investigaciones en Mecánica Teórica y Aplicada, Universidad Tecnológica Nacional - F.R.B.B., 11 de Abril 461, Bahá Blanca, BA, B8000LMI, Argentina, mpiovan@frbb.utn.edu.ar, http://www.frbb.utn.edu.ar*

Keywords: Nonlocal elasticity, Frequency analysis, Nanosensors, biomolecules, boundary conditions.

Abstract. Nanosensors are simple engineering devices designed to detect and convey informations about nanoparticles and biomolecules. The nanosized mass sensors are based on the fact that the resonant frequency is sensitive to the resonator and the attached mass. The change of the attached mass on the resonator causes the resonant frequency to deviate from its original value. The key challenge in mass detection is in quantifying the changes in the resonant frequencies due to the added masses. The present note deals with the variational problem of the nanotube bounded at the ends, with translational and elastic constraints, and attached mass, located in a generic position. Closed-form non local frequency expression is derived; the resonant frequencies and corresponding shift frequencies are calculated and numerical results for different boundary conditions are illustrated.

1 INTRODUCTION

Carbon nanotubes (CNTs) constitute a prominent example of nanomaterials and nanostructures and their discovery by Iijima (1991), has stimulated several studies in nanotechnology applications and nano-scale engineering materials. The extraordinary mechanical and physical properties in addition to the large aspect ratio and low density have made carbon nanotubes (CNTs) ideal components of nanodevices. As a result, progressive research activities regarding CNTs have been ongoing in recent years and there is a wide range of applications, as nanooscillators, nanoelectronics, nanocomposites and nanosensors, in which the vibrational characteristics of CNTs are significant. Moreover, such features make CNTs promising candidates for resolution mass sensor and several studies have investigated the use of CNTs as a mass sensor (Jensen et al., 2008). For example Wu et al. (2006) investigated the resonant frequency and mode shapes of a single-walled carbon nanotube (SWCNT) based mass sensor.

Mechanical behaviors of single-walled carbon nanotubes (SWCNTs) or multi-walled carbon nanotubes (MWCNTs) have been the subject of numerous recent studies. Due to the discreteness of nanostructures, atomistic methods such as molecular dynamics theory are generally applied to study the structural behavior of nanostructures and many researchers have explored the potential of using single-walled carbon nanotubes (SWCNTs) as nanomechanical resonators in atomic scale as shown in Joshi et al. (2010) and Mehdipour et al. (2011). Multiwalled carbon nanotubes (MWCNTs) resonators are easier to manipulate and they have different mechanical structures than SWCNTs ones, due to the interaction between the nanotubes such as the van der Waals (vdW) force and since they are both longer and have largers diameters than SWCNTs. Georgantzinos and Anifantis (2010) predicted the vibrational behavior of single and multiwalled carbon nanotubes when a nanoparticle is attached to them by using a spring-mass-based finite element formulation. Elishakoff et al. (2011) studied the vibrations of a cantilever double-walled carbon nanotubes (DWCNTs) with attached bacterium and the effective stiffness and mass of a DWCNT mass sensor. Mateiu et al. (2005) developed an approach for building a mass sensor based on MWCNTs. Kang et al. (2009) and Kang et al. (2011) examined frequency change of frequency nanomechanical resonators based on DWCNTs with different wall lengths employing molecular dynamics simulations. De Rosa and Lippiello (2014a) developed two different numerical approaches to detect the free vibration frequencies of coaxial DWCNTs: the CDM method and the optimized version of the classical Rayleigh quotient.

Owing to the difficulty of controlled experiments on the nanoscale, and the great difficulty of molecular dynamics (MD) simulations, especially for large-scale systems, continuum mechanical models have been effectively used to study mechanical behaviors of CNTs. For example, the classical Euler-Bernoulli beam theory was employed to model a nanomechanical resonator (Elishakoff and Pentaras, 2009; Elishakoff et al., 2011). Although the classical continuum theory is able to predict the behaviors of nanostructures, it is found to be inadequate because of ignoring the small size effects. Recently, nonlocal elastic continuum models have been used for studying the mechanical behaviour of CNTs including beam models. Their application to the analysis of CNTs allows to evaluate of the small-scale effects influence. Along this line, Lee et al. (2010) used the nonlocal Euler-Bernoulli beam theory to analyze the frequency shift of carbon nanotube based upon mass-sensors.

Nanosensors are simple engineering devices designed to detect and convey informations about nanoparticles and biomolecules. The nanosized mass sensors are based on the fact that the resonant frequency is sensitive to the resonator and the attached mass. The change of the attached mass on the resonator causes the resonant frequency to deviate from its original value.

The key challenge in mass detection is in quantifying the changes in the resonant frequencies due to the added masses. Recently, mass detection based on the resonating nanomechanical tools has been subject of growing interests as for example in Chowdhury et al. (2009) and Murmu and Adhikari (2012). This paper makes the effort to study the resonant frequencies of a SWCNT with an attached nanoparticle, and nonlocal elasticity theory is applied to analyze the vibrational behavior. In Adhikari and Chowdhury (2010), the Authors examined the potential of single-walled CNTs as biosensors using a continuum mechanics-based approach and derived a closed-form expression to calculate the mass of biological objects from the frequency shift. The present note deals with the variational problem of the nanotube bounded at the ends, with translational and elastic constraints, and attached mass, located in a generic position. Closed-form nonlocal frequency expression is derived; the resonant frequencies and corresponding shift frequencies are calculated and numerical results for different boundary conditions are illustrated.

2 ANALYSIS OF THE PROBLEM

Let us consider a cantilever nano-tube (Fig. 1) with span L, cross sectional area A, second moment of area I, Young modulus E, mass density ρ and distributed added mass M located between $\gamma_1 L$ and $\gamma_2 L$.

The nano-tube is supposed to be constrained at the ends by elastically flexible springs, with transverse stiffness k_{TL} and rotational stiffness k_{RL} at left and transverse stiffness k_{TR} and rotational stiffness k_{RR} at right.

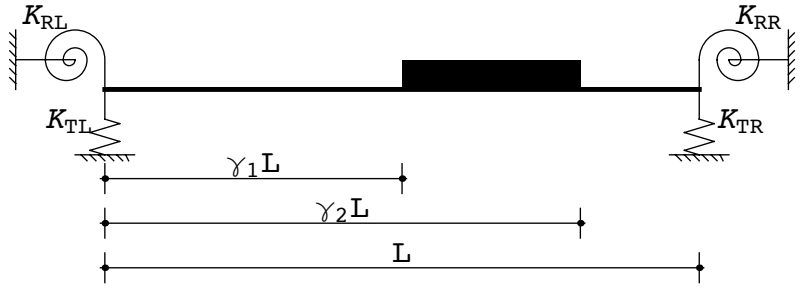

Figure 1: Geometrical properties of the nanotube

According to Hamilton Principle it is possible to write:

$$\int_{t_1}^{t_2} (\delta\,\mathrm{T}(t) - \delta E(t))\,\mathrm{dt} = 0 \tag{1}$$

where

$$\begin{aligned} T = \; & \frac{1}{2}\int_0^{\gamma_1 L} \rho A \left(\frac{\partial v_1(z,t)}{\partial t}\right)^2 \mathrm{dz} + \frac{1}{2}\int_{\gamma_1 L}^{\gamma_2 L} \rho A \left(\frac{\partial v_2(z,t)}{\partial t}\right)^2 \mathrm{dz} + \\ & \frac{1}{2}\int_{\gamma_2 L}^{L} \rho A \left(\frac{\partial v_3(z,t)}{\partial t}\right)^2 \mathrm{dz} + \frac{1}{2}\int_{\gamma_1 L}^{\gamma_2 L} M \left(\frac{\partial v_2(z,t)}{\partial t}\right)^2 \mathrm{dz} \end{aligned} \tag{2}$$

is the kinetic energy of the structure. It is given by the sum of the kinetic energies of the three sections, and of the kinetic energy of the additional mass (Fig. 1). The three displacements functions v_1, v_2 and v_3 vary between $(0, \gamma_1 L)$, $(\gamma_1 L, \gamma_2 L)$, and $(\gamma_2 L, L)$, respectively. The total

potential energy can be expressed as:

$$E = L - P = \frac{1}{2}\int_0^{\gamma_1 L} \mathrm{EI}\left(\frac{\partial^2 v_1(z,t)}{\partial z^2}\right)^2 \mathrm{d}z + \frac{1}{2}\int_{\gamma_1 L}^{\gamma_2 L} \mathrm{EI}\left(\frac{\partial^2 v_2(z,t)}{\partial z^2}\right)^2 \mathrm{d}z + \frac{1}{2}\int_{\gamma_2 L}^{L} \mathrm{EI}\left(\frac{\partial^2 v_3(z,t)}{\partial z^2}\right)^2 \mathrm{d}z + \frac{1}{2}k_{\mathrm{TL}} v_1^2(0,t) + \frac{1}{2}k_{\mathrm{RL}}\left(\frac{\partial v_1(0,t)}{\partial z}\right)^2 + \frac{1}{2}k_{\mathrm{TR}} v_3^2(L,t) + \frac{1}{2}k_{\mathrm{RR}}\left(\frac{\partial v_3(L,t)}{\partial z}\right)^2 - \int_0^{\gamma_1 L} \rho A \frac{\partial^2 v_1(z,t)}{\partial t^2}\eta^2 \frac{\partial^2 v_1(z,t)}{\partial z^2}\,\mathrm{d}z - \int_{\gamma_1 L}^{\gamma_2 L} \rho A \frac{\partial^2 v_2(z,t)}{\partial t^2}\eta^2 \frac{\partial^2 v_2(z,t)}{\partial z^2}\,\mathrm{d}z - \int_{\gamma_2 L}^{L} \rho A \frac{\partial^2 v_3(z,t)}{\partial t^2}\eta^2 \frac{\partial^2 v_3(z,t)}{\partial z^2}\,\mathrm{d}z \tag{3}$$

where L is the sum of the strain energy of the nanotube and of the four strain energies of the elastically flexible springs, P is the potential energy of the inertial force $\left(\rho A \frac{\partial^2 v(z,t)}{\partial t^2}\right)$ due to the additional displacement $(e_0 a)^2 \frac{\partial^2 v(z,t)}{\partial z^2}$ (De Rosa and Lippiello, 2014b), where e_0 is a constant which has to be experimentally determined for each material, a is an internal characteristic length. In that following, one sets $\eta = (e_0 a)$.

The first variation of these two energies can be easily calculated as, so that (1) gives:

$$\int_{t_1}^{t_2}\Big(\int_0^{\gamma_1 L} \rho A \frac{\partial v_1(z,t)}{\partial t}\delta\frac{\partial v_1(z,t)}{\partial t}\,\mathrm{d}z + \int_{\gamma_1 L}^{\gamma_2 L} \rho A \frac{\partial v_2(z,t)}{\partial t}\delta\frac{\partial v_2(z,t)}{\partial t}\,\mathrm{d}z + \int_{\gamma_2 L}^{L} \rho A \frac{\partial v_3(z,t)}{\partial t}\delta\frac{\partial v_3(z,t)}{\partial t}\,\mathrm{d}z + \frac{1}{2}\int_{\gamma_1 L}^{\gamma_2 L} M \frac{\partial v_2(z,t)}{\partial t}\delta\frac{\partial v_2(z,t)}{\partial t}\,\mathrm{d}z - \int_0^{\gamma_1 L}\left(EI\frac{\partial^2 v_1(z,t)}{\partial z^2}\delta\frac{\partial^2 v_1(z,t)}{\partial z^2} - \eta^2\rho A\frac{\partial^2 v_1(z,t)}{\partial t^2}\delta\frac{\partial^2 v_1(z,t)}{\partial z^2}\right)\mathrm{d}z - \int_{\gamma_1 L}^{\gamma_2 L}\left(EI\frac{\partial^2 v_2(z,t)}{\partial z^2}\delta\frac{\partial^2 v_2(z,t)}{\partial z^2} - \eta^2\rho A\frac{\partial^2 v_2(z,t)}{\partial t^2}\delta\frac{\partial^2 v_2(z,t)}{\partial z^2}\right)\mathrm{d}z - \int_{\gamma_2 L}^{L}\left(EI\frac{\partial^2 v_3(z,t)}{\partial z^2}\delta\frac{\partial^2 v_3(z,t)}{\partial z^2} - \eta^2\rho A\frac{\partial^2 v_3(z,t)}{\partial t^2}\delta\frac{\partial^2 v_3(z,t)}{\partial z^2}\right)\mathrm{d}z - k_{\mathrm{TL}} v_1(0,t)\delta v_1(0,t) - k_{\mathrm{RL}}\frac{\partial v_1(0,t)}{\partial z}(0,t)\delta\frac{\partial v_1(0,t)}{\partial z} - k_{\mathrm{TR}} v_3(L,t)\delta v_3(L,t) - k_{\mathrm{RR}}\frac{\partial v_3(L,t)}{\partial z}\delta\frac{\partial v_3(L,t)}{\partial z}\Big)\mathrm{d}t = 0 \tag{4}$$

All the terms in (4) should be integrated by parts, as follows:

$$\int_0^{\gamma_1 L}\int_{t_1}^{t_2}\rho A\frac{\partial v_1(z,t)}{\partial t}\delta\frac{\partial v_1(z,t)}{\partial t}\,\mathrm{dt} = \int_0^{\gamma_1 L}\left[\rho A\frac{\partial v_1(z,t)}{\partial t}\delta v_1(z,t)\right]_{t_1}^{t_2}\mathrm{dz} -$$
$$\int_0^{\gamma_1 L}\int_{t_1}^{t_2}\rho A\frac{\partial^2 v_1(z,t)}{\partial t^2}\delta v_1(z,t)\,\mathrm{dt}\,\mathrm{dz};$$
$$\int_{\gamma_1 L}^{\gamma_2 L}\int_{t_1}^{t_2}\rho A\frac{\partial v_2(z,t)}{\partial t}\delta\frac{\partial v_2(z,t)}{\partial t}\,\mathrm{dt} = \int_{\gamma_1 L}^{\gamma_2 L}\left[\rho A\frac{\partial v_2(z,t)}{\partial t}\delta \mathrm{v}_2(z,t)\right]_{t_1}^{t_2}\mathrm{dz} -$$
$$\int_{\gamma_1 L}^{\gamma_2 L}\int_{t_1}^{t_2}\rho A\frac{\partial^2 v_2(z,t)}{\partial t^2}\delta v_2(z,t)\,\mathrm{dt}\,\mathrm{dz};$$
$$\int_{\gamma_2 L}^{L}\int_{t_1}^{t_2}\rho A\frac{\partial v_3(z,t)}{\partial t}\delta\frac{\partial v_3(z,t)}{\partial t}\,\mathrm{dt}\,\mathrm{dz} = \int_{\gamma_2 L}^{L}\left[\rho A\frac{\partial v_3(z,t)}{\partial t}\delta v_3(z,t)\right]_{t_1}^{t_2}\mathrm{dz} -$$
$$\int_{\gamma_2 L}^{L}\int_{t_1}^{t_2}\rho A\frac{\partial^2 v_3(z,t)}{\partial t^2}\delta v_3(z,t)\,\mathrm{dt}\,\mathrm{dz};$$
$$\int_{\gamma_1 L}^{\gamma_2 L}\int_{t_1}^{t_2}M\frac{\partial v_2(z,t)}{\partial t}\delta\frac{\partial v_2(z,t)}{\partial t}\,\mathrm{dt}\,\mathrm{dz} = \int_{\gamma_1 L}^{\gamma_2 L}\left[M\frac{\partial v_2(z,t)}{\partial t}\delta v_2(z,t)\right]_{t_1}^{t_2}\mathrm{dz} -$$
$$\int_{\gamma_1 L}^{\gamma_2 L}\int_{t_1}^{t_2}M\frac{\partial^2 v_2(z,t)}{\partial t^2}\delta v_2(z,t)\,\mathrm{dt}\,\mathrm{dz}; \tag{5}$$

$$\int_{t_1}^{t_2}\int_0^{\gamma_1 L}\eta^2\rho A\frac{\partial^2 v_1(z,t)}{\partial t^2}\delta\frac{\partial^2 v_1(z,t)}{\partial z^2}\,\mathrm{dz}\,\mathrm{dt} = \int_{t_1}^{t_2}\left[\eta^2\rho A\frac{\partial^2 v_1(z,t)}{\partial t^2}\delta\frac{\partial v_1(z,t)}{\partial z}\right]_0^{\gamma_1 L}\mathrm{dt} -$$
$$\int_{t_1}^{t_2}\left[\eta^2\rho A\frac{\partial^3 v_1(z,t)}{\partial t^2\partial z}\delta v_1(z,t)\right]_0^{\gamma_1 L}\mathrm{dt} + \int_{t_1}^{t_2}\int_0^{\gamma_1 L}\eta^2\rho A\frac{\partial^4 v_1(z,t)}{\partial t^2\partial z^2}\delta v_1(z,t)\,\mathrm{dz}\,\mathrm{dt}; \tag{6}$$

$$\int_{t_1}^{t_2}\int_{\gamma_1 L}^{\gamma_2 L}\eta^2\rho A\frac{\partial^2 v_2(z,t)}{\partial t^2}\delta\frac{\partial^2 v_2(z,t)}{\partial z^2}\,\mathrm{dz}\,\mathrm{dt} = \int_{t_1}^{t_2}\left[\eta^2\rho A\frac{\partial^2 v_2(z,t)}{\partial t^2}\delta\frac{\partial v_2(z,t)}{\partial z}\right]_{\gamma_1 L}^{\gamma_2 L}\mathrm{dt} -$$
$$\int_{t_1}^{t_2}\left[\eta^2\rho A\frac{\partial^3 v_2(z,t)}{\partial t^2\partial z}\delta v_2(z,t)\right]_{\gamma_1 L}^{\gamma_2 L}\mathrm{dt} + \int_{t_1}^{t_2}\int_{\gamma_1 L}^{\gamma_2 L}\eta^2\rho A\frac{\partial^4 v_2(z,t)}{\partial t^2\partial z^2}\delta v_2(z,t)\,\mathrm{dz}\,\mathrm{dt}; \tag{7}$$

$$\int_{t_1}^{t_2}\int_{\gamma_2 L}^{L}\eta^2\rho A\frac{\partial^2 v_3(z,t)}{\partial t^2}\delta\frac{\partial^2 v_3(z,t)}{\partial z^2}\,\mathrm{dz}\,\mathrm{dt} = \int_{t_1}^{t_2}\left[\eta^2\rho A\frac{\partial^2 v_3(z,t)}{\partial t^2}\delta\frac{\partial v_3(z,t)}{\partial z}\right]_{\gamma_2 L}^{L}\mathrm{dt} -$$
$$\int_{t_1}^{t_2}\left[\eta^2\rho A\frac{\partial^3 v_3(z,t)}{\partial t^2\partial z}\delta v_3(z,t)\right]_{\gamma_2 L}^{L}\mathrm{dt} + \int_{t_1}^{t_2}\int_{\gamma_2 L}^{L}\eta^2\rho A\frac{\partial^4 v_3(z,t)}{\partial t^2\partial z^2}\delta v_3(z,t)\,\mathrm{dz}\,\mathrm{dt}; \tag{8}$$

and:

$$-\int_{t_1}^{t_2}\int_0^{\gamma_1 L}\mathrm{EI}\,\frac{\partial^2 v_1(z,t)}{\partial z^2}\delta\frac{\partial^2 v_1(z,t)}{\partial z^2}\,\mathrm{dz}\,\mathrm{dt} = -\int_{t_1}^{t_2}\left[\mathrm{EI}\,\frac{\partial^2 v_1(z,t)}{\partial z^2}\delta\frac{\partial v_1(z,t)}{\partial z}\right]_0^{\gamma_1 L}\mathrm{dt} +$$
$$\int_{t_1}^{t_2}\left[\mathrm{EI}\,\frac{\partial^3 v_1(z,t)}{\partial z^3}\delta v_1(z,t)\right]_0^{\gamma_1 L}\mathrm{dt} - \int_{t_1}^{t_2}\int_0^{\gamma_1 L}\mathrm{EI}\,\frac{\partial^4 v_1(z,t)}{\partial z^4}\delta v_1(z,t)\,\mathrm{dz}\,\mathrm{dt}; \tag{9}$$

$$-\int_{t_1}^{t_2}\int_{\gamma_1 L}^{\gamma_2 L} \mathrm{EI}\,\frac{\partial^2 v_2(z,t)}{\partial z^2}\delta\frac{\partial^2 v_2(z,t)}{\partial z^2}\,\mathrm{dz}\,\mathrm{dt} = -\int_{t_1}^{t_2}\left[\mathrm{EI}\,\frac{\partial^2 v_2(z,t)}{\partial z^2}\delta\frac{\partial v_2(z,t)}{\partial z}\right]_{\gamma_1 L}^{\gamma_2 L}\mathrm{dt} + \int_{t_1}^{t_2}\left[\mathrm{EI}\,\frac{\partial^3 v_2(z,t)}{\partial z^3}\delta v_2(z,t)\right]_{\gamma_1 L}^{\gamma_2 L}\mathrm{dt} - \int_{t_1}^{t_2}\int_{\gamma_1 L}^{\gamma_2 L}\mathrm{EI}\,\frac{\partial^4 v_2(z,t)}{\partial z^4}\delta v_2(z,t)\,\mathrm{dz}\,\mathrm{dt}, \tag{10}$$

$$-\int_{t_1}^{t_2}\int_{\gamma_2 L}^{L} \mathrm{EI}\,\frac{\partial^2 v_3(z,t)}{\partial z^2}\delta\frac{\partial^2 v_3(z,t)}{\partial z^2}\,\mathrm{dz}\,\mathrm{dt} = -\int_{t_1}^{t_2}\left[EI\frac{\partial^2 v_3(z,t)}{\partial z^2}\delta\frac{\partial v_3(z,t)}{\partial z}\right]_{\gamma_2 L}^{L}\mathrm{dt} + \int_{t_1}^{t_2}\left[\mathrm{EI}\,\frac{\partial^3 v_3(z,t)}{\partial z^3}\delta v_3(z,t)\right]_{0}^{L}\mathrm{dt} - \int_{t_1}^{t_2}\int_{\gamma_2 L}^{L}\mathrm{EI}\,\frac{\partial^4 v_3(z,t)}{\partial z^4}\delta v_3(z,t)\,\mathrm{dz}\,\mathrm{dt}\,. \tag{11}$$

Finally, a system of three equations of motion can be defined:

$$\begin{aligned}
&\mathrm{EI}\,\frac{\partial^4 v_1(z,t)}{\partial z^4} - \eta^2\rho A\frac{\partial^4 v_1(z,t)}{\partial z^2\partial t^2} + \rho A\frac{\partial^2 v_1(z,t)}{\partial t^2} = 0,\ 0 < z < \gamma_1 L\\
&\mathrm{EI}\,\frac{\partial^4 v_2(z,t)}{\partial z^4} - \eta^2\rho A\frac{\partial^4 v_2(z,t)}{\partial z^2\partial t^2} + (\rho A + M)\frac{\partial^2 v_2(z,t)}{\partial t^2} = 0, \gamma_1 L < z < \gamma_2 L\\
&\mathrm{EI}\,\frac{\partial^4 v_3(z,t)}{\partial z^4} - \eta^2\rho A\frac{\partial^4 v_3(z,t)}{\partial z^2\partial t^2} + \rho A\frac{\partial^2 v_3(z,t)}{\partial t^2} = 0, \gamma_2 L < z < L;
\end{aligned} \tag{12}$$

together with the following general boundary conditions:

$$-\mathrm{EI}\,\frac{\partial^3 v_1(0,t)}{\partial z^3} + \eta^2\rho A\frac{\partial^3 v_1(0,t)}{\partial t^2\partial z} - k_{TL}v_1(0,t) = 0. \tag{13}$$

$$\mathrm{EI}\,\frac{\partial^2 v_1(0,t)}{\partial z^2} - \eta^2\rho A\frac{\partial^2 v_1(0,t)}{\partial t^2} - k_{RL}\frac{\partial v_1(0,t)}{\partial z} = 0 \tag{14}$$

for $z = 0$ and for $z = L$:

$$\mathrm{EI}\,\frac{\partial^3 v_3(L,t)}{\partial z^3} - \eta^2\rho A\frac{\partial^3 v_3(L,t)}{\partial t^2\partial z} - k_{\mathrm{TR}}v_3(L,t) = 0 \tag{15}$$

$$-\mathrm{EI}\,\frac{\partial^2 v_3(L,t)}{\partial z^2} + \eta^2\rho A\frac{\partial^2 v_3(L,t)}{\partial t^2} - k_{\mathrm{RR}}\frac{\partial v_3(L,t)}{\partial z} = 0 \tag{16}$$

The boundary conditions for $z = \gamma_1 L$ are:

$$\begin{aligned}
v_1(\gamma_1 L,t) &= v_2(\gamma_1 L,t)\\
\frac{\partial v_1(\gamma_1 L,t)}{\partial z} &= \frac{\partial v_2(\gamma_1 L,t)}{\partial z}\\
\eta^2\rho A\frac{\partial^3 v_1(\gamma_1 L,t)}{\partial t^2\partial z} - \mathrm{EI}\,\frac{\partial^3 v_1(\gamma_1 L,t)}{\partial z^3} - \eta^2\rho A\frac{\partial^3 v_2(\gamma_1 L,t)}{\partial t^2\partial z} + \mathrm{EI}\,\frac{\partial^3 v_2(\gamma_1 L,t)}{\partial z^3} &= 0\\
\eta^2\rho A\frac{\partial^2 v_1(\gamma_1 L,t)}{\partial t^2} - EI\frac{\partial^2 v_1(\gamma_1 L,t)}{\partial z^2} - \eta^2\rho A\frac{\partial^2 v_2(\gamma_1 L,t)}{\partial t^2} + \mathrm{EI}\,\frac{\partial^2 v_2(\gamma_1 L,t)}{\partial z^2} &= 0
\end{aligned} \tag{17}$$

and at $z = \gamma_2 L$:

$$
\begin{aligned}
v_2\left(\gamma_2 L, t\right) &= v_3\left(\gamma_2 L, t\right) \\
\frac{\partial v_2\left(\gamma_2 L, t\right)}{\partial z} &= \frac{\partial v_3\left(\gamma_2 L, t\right)}{\partial z} \\
\eta^2 \rho A \frac{\partial^3 v_2\left(\gamma_2 L, t\right)}{\partial t^2 \partial z} - \mathrm{EI}\,\frac{\partial^3 v_2\left(\gamma_2 L, t\right)}{\partial z^3} - \eta^2 \rho A \frac{\partial^3 v_3\left(\gamma_2 L, t\right)}{\partial t^2 \partial z} + EI \frac{\partial^3 v_3\left(\gamma_2 L, t\right)}{\partial z^3} &= 0 \\
+\eta^2 \rho A \frac{\partial^2 v_2\left(\gamma_2 L, t\right)}{\partial t^2} - EI \frac{\partial^2 v_2\left(\gamma_2 L, t\right)}{\partial z^2} - \eta^2 \rho A \frac{\partial^2 v_3\left(\gamma_2 L, t\right)}{\partial t^2} + EI \frac{\partial^2 v_3\left(\gamma_2 L, t\right)}{\partial z^2} &= 0
\end{aligned} \tag{18}
$$

The solutions of equations (12) can be expressed as:

$$
v_h(z,t) = v_h(z) e^{i\omega t},\ h = 1, 2, 3 \tag{19}
$$

The non-dimensional abscissa $\zeta = \frac{z}{L}$ can be introduced, so that the three equations of motion (12) become:

$$
\begin{aligned}
&\frac{\partial^4 v_1}{\partial \zeta^4} + \eta^2 \Omega^4 \frac{\partial^2 v_1}{\partial \zeta^2} - \Omega^4 v_1 = 0 && \text{for} \quad 0 < \zeta < \gamma_1 \\
&\frac{\partial^4 v_2}{\partial \zeta^4} + \eta^2 \Omega^4 \frac{\partial^2 v_2}{\partial \zeta^2} - (1+\lambda)\Omega^4 v_2 = 0 && \text{for} \quad \gamma_1 < \zeta < \gamma_2 \\
&\frac{\partial^4 v_3}{\partial \zeta^4} + \eta^2 \Omega^4 \frac{\partial^2 v_3}{\partial \zeta^2} - \Omega^4 v_3 = 0 && \text{for} \quad \gamma_2 < \zeta < 1
\end{aligned} \tag{20}
$$

with:

$$
m = \rho A; \quad \lambda = \frac{M}{m}; \quad \mu = \frac{\eta}{L}; \quad \Omega = \sqrt{\sqrt{\frac{\omega^2 m L^4}{\mathrm{EI}}}} \tag{21}
$$

The boundary conditions in the presence of constraints are given by:

$$
\begin{aligned}
-\frac{\partial^3 v_1(0)}{\partial \zeta^3} - \mu^2 \Omega^4 \frac{\partial v_1(0)}{\partial \zeta} - K_{\mathrm{TL}} v_1(0) &= 0 \\
\frac{\partial^2 v_1(0)}{\partial \zeta^2} + \mu^2 \Omega^4 v_1(0) - K_{\mathrm{RL}} \frac{\partial v_1(0)}{\partial z} &= 0
\end{aligned} \tag{22}
$$

$$
\begin{aligned}
v_1\left(\gamma_1\right) &= v_2\left(\gamma_1\right) \\
\frac{\partial v_1}{\partial \zeta}\left(\gamma_1\right) &= \frac{\partial v_2}{\partial \zeta}\left(\gamma_1\right) \\
\mu^2 \Omega^4 \frac{\partial v_1\left(\gamma_1\right)}{\partial \zeta} + \frac{\partial^3 v_1\left(\gamma_1\right)}{\partial \zeta^3} - \mu^2 \Omega^4 \frac{\partial v_2\left(\gamma_1\right)}{\partial \zeta} - \frac{\partial^3 v_2\left(\gamma_1\right)}{\partial \zeta^3} &= 0 \\
\mu^2 \Omega^4 v_1\left(\gamma_1\right) + \frac{\partial^2 v_1\left(\gamma_1\right)}{\partial \zeta^2} - \mu^2 \Omega^4 v_2\left(\gamma_1\right) - \frac{\partial^2 v_2\left(\gamma_1\right)}{\partial \zeta^2} &= 0
\end{aligned} \tag{23}
$$

$$
\begin{aligned}
v_2(\gamma_2) &= v_3(\gamma_2) \\
\frac{\partial v_2}{\partial \zeta}(\gamma_2) &= \frac{\partial v_3}{\partial \zeta}(\gamma_2) \\
\mu^2\Omega^4 \frac{\partial v_2(\gamma_2)}{\partial \zeta} + \frac{\partial^3 v_2(\gamma_2)}{\partial \zeta^3} - \mu^2\Omega^4 \frac{\partial v_3(\gamma_2)}{\partial \zeta} - 1\frac{\partial^3 v_3(\gamma_2)}{\partial \zeta^3} &= 0 \\
\mu^2\Omega^4 v_2(\gamma_2) + \frac{\partial^2 v_2(\gamma_2)}{\partial \zeta^2} - \mu^2\Omega^4 v_3(\gamma_2) - \frac{\partial^2 v_3(\gamma_2)}{\partial \zeta^2} &= 0
\end{aligned} \tag{24}
$$

$$
\begin{aligned}
\frac{\partial^3 v_3(1)}{\partial \zeta^3} + \mu^2\Omega^4 \frac{\partial v_3(1)}{\partial \zeta} - K_{\mathrm{TR}} v_3(1) &= 0 \\
-\frac{\partial^2 v_3(1)}{\partial \zeta^2} - \mu^2\Omega_1^4 v_3(1) - K_{\mathrm{RR}} \frac{\partial v_3(1)}{\partial z} &= 0
\end{aligned} \tag{25}
$$

where the following non-dimensional stiffness coefficients are defined as:

$$
K_{\mathrm{TL}} = \frac{k_{\mathrm{TL}} L^3}{\mathrm{EI}}; \quad K_{\mathrm{RL}} = \frac{k_{\mathrm{RL}} L}{\mathrm{EI}}; \quad K_{\mathrm{TR}} = \frac{k_{\mathrm{TR}} L^3}{\mathrm{EI}}; \quad K_{\mathrm{RR}} = \frac{k_{\mathrm{RR}} L}{\mathrm{EI}} \tag{26}
$$

The general solutions of these equations are given by:

$$
\begin{aligned}
v_1(z) &= A_1 \cos(\alpha\zeta) + A_2 \sin(\alpha\zeta) + A_3 \cos h(\alpha\zeta) + A_4 \sin h(\alpha\zeta) \\
v_2(z) &= B_1 \cos(\alpha_1\zeta) + B_2 \sin(\alpha_1\zeta) + B_3 \cos h(\beta_1\zeta) + B_4 \sin h(\beta_1\zeta) \\
v_3(z) &= C_1 \cos(\alpha\zeta) + C_2 \sin(\alpha\zeta) + C_3 \cos h(\beta\zeta) + C_4 \sin h(\beta\zeta)
\end{aligned} \tag{27}
$$

with:

$$
\begin{aligned}
\alpha &= \sqrt{\frac{1}{2}\left(\mu^2\Omega^4 + \Omega^2\sqrt{4+\mu^4\Omega^4}\right)}; & \beta &= \sqrt{\frac{1}{2}\left(-\mu^2\Omega^4 + \Omega^2\sqrt{4+\mu^4\Omega^4}\right)}; \\
\alpha_1 &= \sqrt{\frac{1}{2}\left(\mu^2\Omega^4 + \Omega^2\sqrt{4+4\lambda+\mu^4\Omega^4}\right)}; & \beta_1 &= \sqrt{\frac{1}{2}\left(-\mu^2\Omega^4 + \Omega^2\sqrt{4+4\lambda+\mu^4\Omega^4}\right)}
\end{aligned} \tag{28}
$$

The twelve constants can be found by imposing the boundary conditions (23)-(25). The governing system is homogeneous and the non-triviality of the solution requires the coefficients' determinant to be equal to zero. Solution of this equation system yields the desired non-dimensional natural frequencies Ω_i.

2.1 FREQUENCY SHIFT

Once non-dimensional frequencies have been obtained, in particular the first frequency value Ω_1, it is possible to derive the first resonant frequency:

$$
f_1 = \frac{\omega_1}{2\pi} = \frac{\Omega_1^2}{2\pi}\sqrt{\frac{\mathrm{EI}}{mL^4}} \tag{29}
$$

The aim is to derive the added mass value, so that the relative frequency shift is calculated by the following expression:

$$\frac{\Delta f}{f_0} = \frac{f_0 - f_1}{f_0} \tag{30}$$

where f_0 is the resonant frequency of the nano-tube without added mass and neglecting the nonlocal effect.

Known the resonant frequency, in the absence of mass and nonlocal effect, and the resonant frequency in the presence of mass and nonlocal effect, it is possible to derive the relative shift frequency and from theoretical curves $(\lambda\,(\gamma_2 - \gamma_1), \Delta f/f_0)$ the nondimensional mass λ is determined, which in turn makes possible to deduce the M value.

3 NUMERICAL EXAMPLES

Let us consider the clamped free single-walled carbon nano-tube with attached mass, assuming that the nondimensional transverse and rotational stiffness, at left end, are large enough while the non-dimensional transverse and rotational stiffness, at right end, are equal to zero.

Assuming the calibration constants derived from the paper of Adhikari and Chowdhury (2010) and solving the differential equations system given in (20), the numerical comparison is performed. The material and geometrical properties of single-walled carbon nano-tube, so as deduced from the paper Reddy and Pang (2008), are reported in Table 1.

SWCNT properties density	Symbol	Value	Unit
Cross section area	A	$7.85\ 10^{-19}$	m^2
Radius	R	$0.5\ 10^{-9}$	m
Length	L	$9\ 10^{-9}$	m
Moment of inertia	I	$4.91\ 10^{-38}$	m^4
Density	ρ	2300	Kg/m^3
Young's modulus	E	$1000\ 10^9$	Pa

Table 1: Geometrical and material properties of the nano-tube

In this case, one assumes a fixed location of attached mass, at the free end, and setting $\gamma = \gamma_2 - \gamma_1$ and $\gamma_2 = 1$, it is possibile to increase the value of γ varying γ_1.The non-dimensional mass is so defined:

$$\lambda = \frac{M}{m} = 1 \tag{31}$$

The relative frequency shift, as deduced from the work of Adhikari and Chowdhury (2010), is given by the following expression:

$$\frac{\Delta f}{f_0} = 1 - \frac{1}{\sqrt{1 + c_m \lambda}} \tag{32}$$

where c_m is mass calibration constant which is a function of the length of the attached mass $\gamma = (\gamma_2 - \gamma_1)$ as shown in Table 1 of the paper of Adhikari and Chowdhury (2010).

As can be seen in Table 2, with the increase in the value of γ, the relative frequency shift value deduced from the approximate formula approaches the value obtained from the exact solution; whereas for the values of equal to 0.7 and 0.8, the approximate and exact relative frequency shift values coincide.

γ	$\Delta f/f_0$ Adhikari and Chowdhury (2010)	$\Delta f/f_0$
0.1	0.13853	0.13908
0.2	0.20947	0.21007
0.3	0.24918	0.24956
0.4	0.27163	0.27180
0.5	0.28375	0.28380
0.6	0.28965	0.28966
0.7	0.29206	0.29206
0.8	0.29277	0.29277

Table 2: Numerical comparison with the paper of Adhikari and Chowdhury (2010).

In the following numerical examples, one evaluates the influence on the resonant frequency ($f_1 = \frac{\omega_1}{2\pi}$) of nonlocal effect μ for varying values of the length of the attached mass.

For all subsequent examples, the same material and geometrical data, given in Table 1, are adopted. Considering a clamped free nanotube, the first numerical example is performed. As is shown, the clamped free nano-tube represents a peculiar numerical case because it is the single numerical example in which the resonant frequency increases when the nonlocal effect increases. In Table 3 the first resonant frequency f_1 value is reported and the value the lenght of the attached mass varies between 0 and 0.9 and the non local effect values μ are [0, 0.1, 0.3, 0.5].

γ	$\mu = 0$	$\mu = 0.1$	$\mu = 0.3$	$\mu = 0.5$
0	3.60268 10^{10}	3.61834 10^{10}	3.75909 10^{10}	4.18895 10^{10}
0.1	3.10162 10^{10}	3.11245 10^{10}	3.20756 10^{10}	3.46665 10^{10}
0.2	2.84585 10^{10}	2.85418 10^{10}	2.926 10^{10}	3.10933 10^{10}
0.3	2.7036 10^{10}	2.71057 10^{10}	2.77009 10^{10}	2.91661 10^{10}
0.4	2.62348 10^{10}	2.6297 10^{10}	2.68251 10^{10}	2.80985 10^{10}
0.5	2.58023 10^{10}	2.58605 10^{10}	2.63527 10^{10}	2.75263 10^{10}
0.6	2.55911 10^{10}	2.56473 10^{10}	2.6122 10^{10}	2.72473 10^{10}
0.7	2.55048 10^{10}	2.55602 10^{10}	2.60277 10^{10}	2.71335 10^{10}
0.8	2.54791 10^{10}	2.55342 10^{10}	2.59996 10^{10}	2.70995 10^{10}
0.9	2.54749 10^{10}	2.55301 10^{10}	2.59951 10^{10}	2.70941 10^{10}

Table 3: The first resonant frequency value for a clamped free nano-tube and for different values of length γ of the attached mass and nonlocal effect μ

The first four values of the resonant frequency, reported in Table 3 and for $\gamma = 0$, can be compared with those obtained to the formula (163) in the article Reddy and Pang (2008). As one can see, the results are coincident. For the other numerical results, the following considerations apply:

- if (γ λ) increases, the first resonant frequency value decreases;
- if the nonlocal effect non-dimensional parameter increases, the first resonant frequency value increases.

In the following numerical example the supported-supported nano-tube is considered.

γ	$\mu = 0$	$\mu = 0.1$	$\mu = 0.3$	$\mu = 0.5$
0	1.01129 10^{11}	9.64802 10^{10}	7.35945 10^{10}	5.43094 10^{10}
0.1	9.2364 10^{10}	8.87827 10^{10}	7.00047 10^{10}	5.28184 10^{10}
0.2	8.5832 10^{10}	8.29364 10^{10}	6.70323 10^{10}	5.15073 10^{10}
0.3	8.0997 10^{10}	7.85503 10^{10}	6.46528 10^{10}	5.04043 10^{10}
0.4	7.74741 10^{10}	7.53245 10^{10}	6.28171 10^{10}	4.95195 10^{10}
0.5	7.49823 10^{10}	7.30279 10^{10}	6.14649 10^{10}	4.88483 10^{10}
0.6	7.33083 10^{10}	7.14784 10^{10}	6.05314 10^{10}	4.83752 10^{10}
0.7	7.22794 10^{10}	7.05235 10^{10}	5.99475 10^{10}	4.80753 10^{10}
0.8	7.17408 10^{10}	7.00229 10^{10}	5.9639 10^{10}	4.79156 10^{10}
0.9	7.15385 10^{10}	6.98347 10^{10}	5.95225 10^{10}	4.78552 10^{10}

Table 4: The first resonant frequency value for a supported-supported nanotube and for different values of length γ of the attached mass and nonlocal effect μ.

In Table 4 the resonant frequency values, varying the length of the attached mass and nonlocal effect, are reported. The added mass is located at midpoint of length of the nano-tube and for this case, for example for $\gamma = 0.1$, γ_1 and γ_2 are equal 0.45 and 0.55, respectively.

It is seen that the resonant frequency parameter of SWCNT decreases with increasing the length of the attached mass and the nonlocal effect parameter.

This circumstance show that when one consider the boundary conditions different from cantilever case, the nonlocal effect plays a beneficial effect on the first resonant frequency.

Using the Tables 3 and 4, it is possible deduce the relative frequency shift (30) and plot the theoretical curves $(\lambda\gamma, \Delta f/f_0)$, varying μ. The curves $(\lambda\gamma, \Delta f/f_0)$ are also useful to derive the added mass value M (Adhikari and Chowdhury, 2010).

In the last numerical example, a nano-tube clamped at left and with the right side constrained by an elastically flexible translation spring is considered, with non-dimensional stiffness coefficient $K_{\rm TR}$, as given in (26). The distributed mass is located at the midpoint of nanotube, for $\gamma = 0.2$, $\gamma_1 = 0.4$ and $\gamma_2 = 0.6$, respectively.

$K_{\rm TR}$	$\mu = 0$	$\mu = 0.1$	$\mu = 0.3$	$\mu = 0.5$
0	3.43856 10^{10}	3.45148 10^{10}	3.56563 10^{10}	3.88546 10^{10}
0.5	3.70214 10^{10}	3.71472 10^{10}	3.82653 10^{10}	4.14612 10^{10}
1	3.945 10^{10}	3.957 10^{10}	4.06439 10^{10}	4.37843 10^{10}
5	5.43556 10^{10}	5.43674 10^{10}	5.45858 10^{10}	5.60502 10^{10}
10	6.70448 10^{10}	6.68313 10^{10}	6.53164 10^{10}	6.34042 10^{10}
50	1.06055 10^{11}	1.03811 10^{11}	8.98243 10^{10}	7.33336 10^{10}
10^2	1.18404 10^{11}	1.14964 10^{11}	9.52284 10^{10}	7.47067 10^{10}
10^3	1.31725 10^{11}	1.2378 10^{11}	1.00433 10^{11}	7.59115 10^{10}
10^4	1.3311 10^{11}	1.28005 10^{11}	1.0096 10^{11}	7.60296 10^{10}
10^5	1.33249 10^{11}	1.28128 10^{11}	1.01012 10^{11}	7.60414 10^{10}
10^{10}	1.33264 10^{11}	1.28141 10^{11}	1.01018 10^{11}	7.60427 10^{10}
10^{15}	1.33264 10^{11}	1.28141 10^{11}	1.01018 10^{11}	7.60427 10^{10}

Table 5: The first resonant frequency value for a clamped free nanotube and constrained by non-dimensional elastically flexible spring $K_{\rm TR}$ at the right end and nonlocal effect μ.

The first numerical results are obtained with non-dimensional transverse stiffness $K_{\rm TR} = 0$.

Increasing the non-dimensional parameter μ and $K_{\rm TR}$, the resonant frequency increases. For $K_{\rm TR}$ within the range $5 < K_{\rm TR} < 10$, the behavior of the nanotube switches from the clamped free behavior, in which increasing values of the coefficient μ lead to increasing resonant frequencies, to the clamped-supported behavior: actually, for higher $K_{\rm TR}$ values the resonant frequency decreases. In this particular case a small nondimensional transverse stiffness do not modify the resonant frequency behavior, with respect to the clamped free nano-tube.

4 CONCLUSIONS

Based on the nonlocal elasticity theory, the free frequencies analysis has been performed for the single-walled nano-tube case, bounded at the ends, with translational and elastic constraints, and attached mass, located in a generic position. The closed-form nonlocal frequency expression has been derived by means of the Hamilton's principle; then the resonant frequency and corresponding shift frequency have been calculated. Numerical results for different boundary conditions have been performed in order to evaluate the effect of the nonlocal coefficient on the first resonant frequency value. The obtained results can be employed for finding the distributed added mass, i.e. from resonant frequency value, in absence of mass and nonlocal effect, and the resonant frequency value, in presence of the mass and nonlocal effect, it is possible to derive the relative frequency shift and from theoretical curves calculate the non-dimensional mass λ and then the relative added mass M.

The present approach can be applied to analyze the dynamic behavior of multi-walled carbon nano-tubes (MWCNTs) and in the case of nano-tubes based upon the Timoshenko theory.

REFERENCES

Adhikari S. and Chowdhury R. The calibration of nanotube based bionanosensors. *Journal of Applied Physics*, 107:124–322, 2010.

Chowdhury R., Adhikari S., and Mitchell J. Vibrating carbon nanotube based bio-sensor. *Physica E*, 42:104–109, 2009.

De Rosa M. and Lippiello M. Free vibration analysis of dwcnts using cdm and rayleigh-schimdt based on nonlocal euler-bernoulli beam theory. *The Scientific World Journal*, 2014a.

De Rosa M. and Lippiello M. Hamilton principle for swcn and a modified approach for nonlocal frequency analysis of nanoscale biosensor. *Nanoletters, under review*, 2014b.

Elishakoff I. and Pentaras D. Fundamental natural frequencies of double-walled carbon nanotubes. *Journal of Sound and Vibration*, 322:652–664, 2009.

Elishakoff I., Versaci C., and Muscolino G. Clamped-free double-walled carbon nanotube-based mass sensor. *Acta Mechanica*, 219:29–43, 2011.

Georgantzinos S. and Anifantis N. Carbon nanotube-based resonant nanomechanical sensors: A computational investigation of their behavior. *Physica E*, 42(5):1795–1801, 2010.

Iijima S. Helical microtubules of graphitic carbon. *Nature*, 354:56–58, 1991.

Jensen K., Kim K., and Zett A. An atomic-resolution nanomechanical mass sensor. *Nature Nanotechnology*, 3:533–537, 2008.

Joshi A., Sharma S., and Harsha S. Dynamic analysis of a clamped wavy single walled carbon nanotube based nanomechanical sensors. *Journal of Nanotechnology in Engineering and Medicine*, 1:031007, 2010.

Kang J., Kwon O., Hwang H., and Jiang Q. Resonance frequency distribution of cantilevered (5,5) (10,10) double-walled carbon nanotube with different intertube lengths. *Molecular Simulation*, 37(1):18–22, 2011.

Kang J., Kwon O., Lee J., Choi Y., and Hwang H. Frequency change by interwalled length difference of double-walled carbon nanotube resonator. *SolidState Communications*, 149(1):1574–1577, 2009.

Lee H., Hs J., and Chang W. Frequency shift of carbon nanotube-based mass sensors using nonlocal elasticity theory. *Nanoscale Research Letters*, 5:1774–1778, 2010.

Mateiu R., Kuhle A., Marie R., and Boisen A. Building a multi-walled carbon nanotube-based mass sensor with the atomic force microscope. *Ultramicroscopy*, 105:233–237, 2005.

Mehdipour I., Barari A., and Domairry G. Application of a cantilevered swcnt with mass at the tip as a nanomechanical sensor. *Computational Material Science*, 50:1830–1833, 2011.

Murmu T. and Adhikari S. Nonlocal frequency analysis of nanoscale biosensors. *Sensors and Actuators A*, 173:41–48, 2012.

Reddy J. and Pang S. Nonlocal continuum theories of beams for the analysis of carbon nanotubes. *Journal of Applied Physics*, 103:023511–26, 2008.

Wu D., Chien W., Chen C., and Chen H. Resonant frequency analysis of fixed-free single-walled carbon nanotube-based mass sensor. *Sensors and Actuators A*, 126:117–121, 2006.